Journal of Power Sources 195 (2010) 8075–8079

Contents lists available at ScienceDirect

Journal of Power Sources

journal homepage: www.elsevier.com/locate/jpowsour

Short communication

Improved stability of TiO_2 modified $Ru_{85}Se_{15}$/C electrocatalyst for proton exchange membrane fuel cells

Ting Xu[a,b], Huamin Zhang[a,*], Hexiang Zhong[a], Yuanwei Ma[a,b], Hong Jin[a,b], Yining Zhang[a]

[a] PEMFC Key Materials and Technology Laboratory, Dalian Institute of Chemical Physics, Chinese Academy of Sciences, Dalian 116023, China
[b] Graduate School of the Chinese Academy of Sciences, Beijing 100039, China

ARTICLE INFO

Article history:
Received 26 June 2010
Accepted 7 July 2010
Available online 13 July 2010

Keywords:
Proton exchange membrane fuel cells
Electrocatalyst
Stability
Titanium dioxide

ABSTRACT

The electrocatalytic stability of the carbon supported $Ru_{85}Se_{15}$ nanoparticles has been improved by the modification of titanium dioxide for proton exchange membrane fuel cells (PEMFCs). Transmission electron microscopy (TEM), X-ray diffraction (XRD) measurements and inductively coupled plasma-atomic emission spectroscopy (ICP-AES) are applied for characterizing $Ru_{85}Se_{15}$/C and titanium dioxide modified $Ru_{85}Se_{15}$/C ($Ru_{85}Se_{15}/TiO_2$/C) electrocatalysts. Electrochemical measurements and single cell tests are conducted for the evaluation of the electrocatalysts. The results indicate that $Ru_{85}Se_{15}/TiO_2$/C electrocatalyst, presenting similar initial oxygen reduction reaction (ORR) activity with $Ru_{85}Se_{15}$/C, reveals better electrochemical stability. The final potential of $Ru_{85}Se_{15}/TiO_2$/C is 137 mV higher than that of $Ru_{85}Se_{15}$/C at 2 mA cm^{-2} after the electrochemical durability test. Moreover, in the single cell stability test $Ru_{85}Se_{15}/TiO_2$/C also shows comparable initial performance with $Ru_{85}Se_{15}$/C, but better final performance. Therefore, the $Ru_{85}Se_{15}$/C is expected to be used as an effective cathode electrocatalyst for PEMFCs by TiO_2 modification on the carbon support.

1. Introduction

Proton exchange membrane fuel cells (PEMFCs) have drawn much attention as devices of power source conversion, attributed to their high efficiency and power density, rapid start up and environmental benignancy. As one of the key materials, carbon supported Pt or Pt-based catalysts, have seriously hindered the commercialization of PEMFCs, due to the prohibitive cost and limited abundance of Pt. Therefore, the search for alternative Pt-free catalysts plays a significant role in the development of PEMFCs.

As one of the most competitive alternatives, Ru-based chalcogenide compounds have intensely been investigated attributed to their excellent catalytic behavior and relatively low cost, which were initially reported as oxygen reduction reaction (ORR) catalysts by Vante et al. [1] in 1986. This kind of compounds was initially synthesized using carbonyl compounds as precursors with high cost under harsh conditions, such as at extremely high temperature (1000–2000 °C) and using high purity reactants [1]. Much work has been conducted on the improvement of synthetic method and replacement of high cost precursors. For example, the Ru_xSe_y compound could be synthesized by a simple method with pyrolysis of the carbonyl complex in inert gas [2]. Also, aqueous route was introduced by Delacôte et al. [3] to prepare Se/Ru(Se)/C catalysts, using $NaBH_4$ as a reducing agent for $RuCl_3$ and SeO_2 in basic media. In our previous work [4] $Ru_{85}Se_{15}$/C catalyst with high catalytic activity was synthesized with low-cost precursors by microwave-assisted polyol process, which was fast, simple and environment friendly. Although the electrochemical activity and preparation cost reduction improvement have been achieved, the stability of the catalysts is still problematic, which hinders the final application of this kind of low-cost non-platinum catalysts.

For the Ru_x catalyst, the active center toward the ORR is believed to be the Ru–Ru bond [5], nevertheless Ru atoms are easily oxidized at relatively low potential [6], which leads to the decrease of the ORR activity of the catalyst. When surrounded by Se atoms, Ru atoms are protected from being oxidized. Therefore, Se is believed to play a significant role in the enhancement of electrocatalytic activity and stability of Ru [6]. However, the stability of Se itself seems dubious. Se begins to strip from Ru core at 0.85 V vs. reversible hydrogen electrode (vs. RHE) [7], and the dissolution of Se on Au electrode takes place in the potential range of 0.66–0.99 V vs. Ag/AgCl. Therefore, a crucial problem for this kind of catalysts is the poor electrochemical stability, especially under high potential.

Titanium dioxide has been employed as supporting materials [8–10], due to its excellent chemical and redox stability and corrosion resistance in the acidic environment. The presence of TiO_2 is likely to avoid the agglomeration of Pt particles, helpful in controlling the catalyst nanostructure and providing thermal and

* Corresponding author. Tel.: +86 411 84379072; fax: +86 411 84665057.
E-mail address: zhanghm@dicp.ac.cn (H. Zhang).

0378-7753/$ – see front matter © 2010 Elsevier B.V. All rights reserved.
doi:10.1016/j.jpowsour.2010.07.019

oxidation stability [9]. TiO_2 has also been employed in other kinds of batteries to improve their electrochemical performance and stability attributed to its high electrochemical stability at elevated temperatures and higher working potentials [11].

In this paper, $Ru_{85}Se_{15}$ supported on carbon black modified by titanium dioxide ($Ru_{85}Se_{15}/TiO_2/C$) was prepared by the novel microwave-assisted polyol synthetic method described in our previous work [4], using the facile precursors of $RuCl_3$ and Na_2SeO_3. To improve the electrochemical stability of $Ru_{85}Se_{15}/C$ catalyst, TiO_2 is added for two intentions. One is to disperse and anchor $Ru_{85}Se_{15}$ nanoparticles in order to prevent them from aggregation. The other is to enhance the electrochemical stability of the catalyst at high potential by preventing Se and Ru from oxidation and loss.

2. Experimental

2.1. Synthesis of the electrocatalysts

The $Ru_{85}Se_{15}/TiO_2/C$ (5 wt.% TiO_2 and 20 wt.% $Ru_{85}Se_{15}$) catalyst was synthesized as follows. The first step was the synthesis of TiO_2/C. 1 g tetra-n-butyl titanate and 6 g trolamine were mixed in 40 mL ethanol, followed by refluxed while stirring at 90 °C in N_2 for 6 h to get $Ti[HOC_2H_4N(OC_2H_4)_2]_2$ (denoted as Ti-2TEA):

$$Ti[CH_3(CH_2)_3O]_4 + 2(HOCH_2CH_2)_3N \rightarrow Ti[HOC_2H_4N(OC_2H_4)_2]_2$$

Then, the solution of Ti-2TEA was diluted with ethanol to 100 mL. 10 mL Ti-2TEA dilution as-prepared was added into homogeneous slurry including 350.4 mg Vulcan XC-72R carbon black (Cabot Corp., $S_{BET} = 250\ m^2\ g^{-1}$) and 60 mL H_2O. The mixture was refluxed while stirring at 90 °C for 1 h after 4 mL of 2 M HNO_3 solution was added. The resulting solid was filtered, and dried in a vacuum oven at 60 °C for 8 h. Subsequently, the sample was heat-treated at 300 °C in the air for 3 h to obtain TiO_2/C powder.

Secondly, with the TiO_2/C powder as-prepared as support, $Ru_{85}Se_{15}/TiO_2/C$ catalyst was prepared using $RuCl_3$ and Na_2SeO_3 as the Ru and Se precursors with microwave-assisted polyol process described in our previous work [4].

For comparison, $Ru_{85}Se_{15}/C$ was synthesized via the same procedure as $Ru_{85}Se_{15}/TiO_2/C$ catalyst with Vulcan XC-72R carbon black as support.

2.2. Physicochemical characterizations

The crystalline structures of Vulcan XC-72R carbon black, TiO_2/C, $Ru_{85}Se_{15}/TiO_2/C$ and $Ru_{85}Se_{15}/C$ were studied using a Rigaku Rotalflex (RU-200B) with Ni filtered Cu-K_α radiation (λ = 1.54056 å). Conventional $2\theta/\theta$ scans (2θ is the Bragg angle) were performed with a scan rate of 5° min^{-1} and a step size of 0.02° within the 2θ angular region from 20° to 85°.

Transmission electron microscopy (TEM) was performed using a JEOL JEM-2000EX microscope operating at 120 kV. The samples were dispersed in ethanol by ultrasonic blending to form homogeneous slurry, which was applied onto a holey carbon-coated copper grid. Two hundreds of particles were calculated to obtain the particle distribution diagram of each catalyst sample.

2.3. Electrochemical measurements

The activities of the samples toward ORR were evaluated by the rotating disk electrode (RDE) method with CHI 600 electrochemical station (CH Corp., USA) coupled with a RDE system (EG&G model 636). All the RDE measurements were carried out in a standard three-electrode cell in 0.5 M H_2SO_4 electrolyte at room temperature, with a saturated calomel electrode (SCE) and a Pt foil (3 cm^2) as reference and counter electrodes, respectively. The working electrode with the catalyst layer on the glassy carbon electrode (GCE, 0.1256 cm^2) was prepared as follows: a mixture containing 5.0 mg of $Ru_{85}Se_{15}/TiO_2/C$ or $Ru_{85}Se_{15}/C$ catalyst, 1 mL ethanol, and 50 μL Nafion (DuPont Corp., 5 wt.%) was ultrasonically blended into a homogenous slurry, 25 μL of which was deposited on a clean GCE surface and dried in air. The RDE tests were obtained in O_2-saturated electrolyte by sweeping the working electrode from 0.95 to 0.1 V vs. RHE at 5 mV s^{-1} with rotation speed of 1600 rpm.

To investigate electrochemical durability of the samples, 1000 cycles of potential cycling accelerated stability test were performed between 0 and 1 V vs. RHE at 50 mV s^{-1} in the N_2-saturated 0.5 M H_2SO_4 solution. Then the final ORR activity was recorded.

In order to determine the loss amounts of Ru and Se for the two catalysts in the electrochemical durability test, inductively coupled plasma-atomic emission spectroscopy (ICP-AES) analysis was conducted on the solution of 0.5 M H_2SO_4 electrolyte after the electrochemical durability test.

2.4. Fabrication of membrane electrode assembly (MEA) and single cell tests

The cathode was prepared as follows: $Ru_{85}Se_{15}/C$ catalyst or $Ru_{85}Se_{15}/TiO_2/C$ was mixed with Nafion (DuPont Corp., 5 wt.%) and ethanol to form homogeneous slurry, which was cast onto the wet-proofed carbon paper (Torry carbon paper, 7 wt.% PTFE). The Ru loading on the electrode was 0.5 mg cm^{-2} and the dry Nafion loading was 0.5 mg cm^{-2}. The anode adopted the commercial 28.4 wt.% Pt/C catalyst (TKK Corp.) with Pt loading of 0.4 mg cm^{-2}. The MEA with 5 cm^2 active area was fabricated by hot-pressing the anode and the cathode to the Nafion 212 membrane (DuPont Corp., 50 μm) at 1 MPa and 140 °C for 1 min. The single cell was tested at 80 °C with over-saturated humidification. Pure hydrogen and oxygen were injected at 0.2 MPa.

2.5. Potential sweep tests

In order to evaluate the durability of cathode catalysts on the cell performances, potential cycling accelerated aging test (AAT) was conducted after recording the initial performance. During the test, the cell was operated with hydrogen on the anode side and nitrogen on the cathode side with over-saturated humidification at 0.2 MPa. A potential cycling between 0.6 and 1.0 V vs. the anode side for 1000 cycles, which was a strict condition to the cathode catalyst, was adopted to subject the cathode side of the cell with a scan rate of 20 mV s^{-1}. Cell performance was investigated after the AAT.

3. Results and discussion

3.1. Physicochemical characterizations of the catalysts

Crystalline phase identifications of samples were carried out by X-ray diffraction (XRD) patterns presented in Fig. 1. Identical with the results of Kao et al. [12], diffraction peaks of TiO_2/C at about 37.8°, 48.0° and 53.9° assigned to the anatase phase of TiO_2 are unambiguously identified. And the diffraction peak at about 43° is assigned to the C (1 0 1). However, other characteristic peaks of TiO_2 in anatase phase are not evident, which may result from the small amount of TiO_2 loading and some of TiO_2 in amorphous structure. As shown in Fig. 1, both the $Ru_{85}Se_{15}/C$ catalyst and $Ru_{85}Se_{15}/TiO_2/C$ catalyst show the crystalline structures of metallic ruthenium (JCPDS Powder Diffraction File No. 06-0663). And crystalline features of the two catalysts are almost the same, indicating that the addition of TiO_2 has no effect on the crystalline lattice of $Ru_{85}Se_{15}$. Furthermore, the diffraction peak at about 44° is assigned to the Ru (1 0 1). The diffraction peaks of the both catalysts shifted

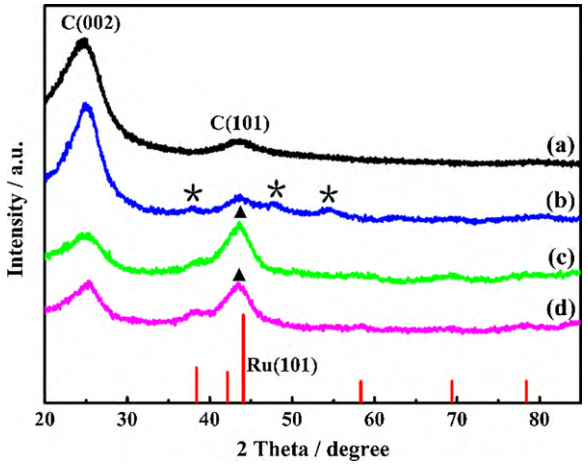

Fig. 1. XRD patterns of (a) Vulcan XC-72R carbon black; (b) as-prepared TiO_2/C; (c) $Ru_{85}Se_{15}/TiO_2$/C catalyst and (d) $Ru_{85}Se_{15}$/C catalyst.

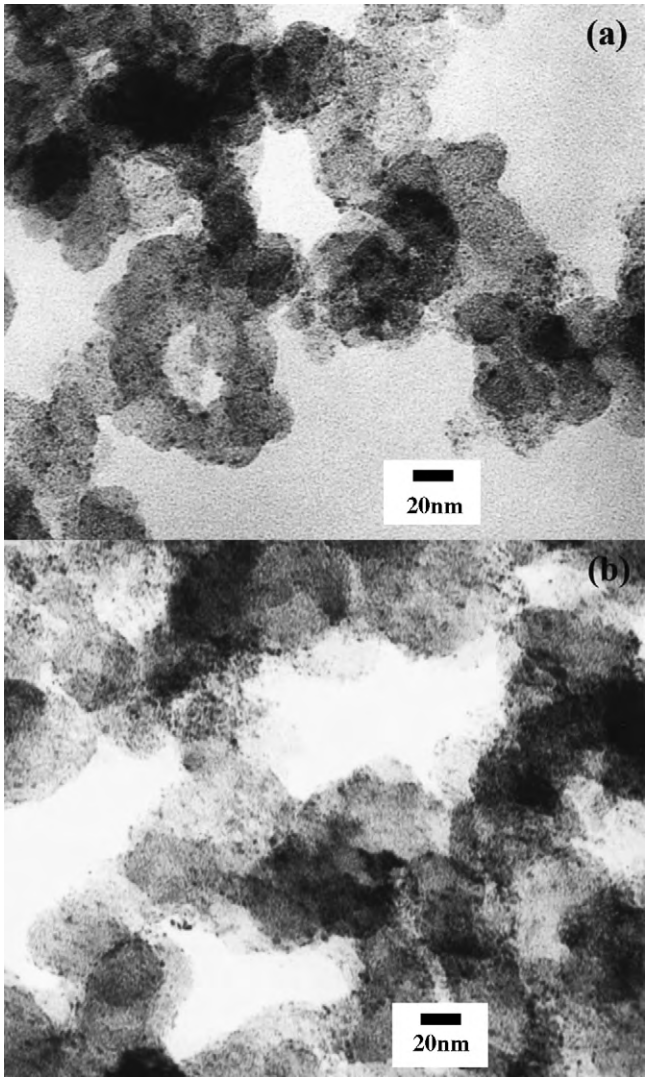

Fig. 2. TEM images of the catalysts before the electrochemical durability test (a) $Ru_{85}Se_{15}$/C catalyst and (b) $Ru_{85}Se_{15}/TiO_2$/C catalyst.

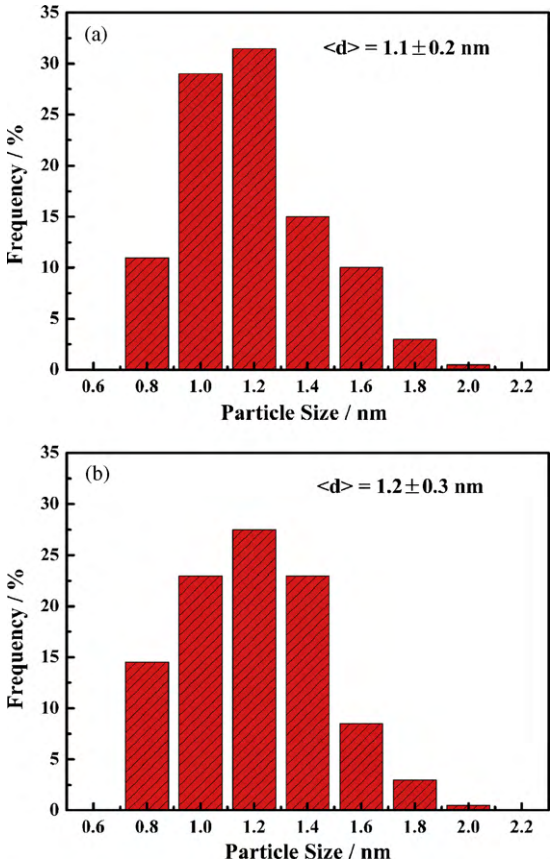

Fig. 3. Histograms of particle size distributions of the catalysts before the electrochemical durability test (a) $Ru_{85}Se_{15}$/C catalyst and (b) $Ru_{85}Se_{15}/TiO_2$/C catalyst.

to a smaller angle compared to the characteristic peaks of Ru due to the addition of Se. The diffraction peaks corresponding to the TiO_2 are not observed in the XRD patterns of $Ru_{85}Se_{15}/TiO_2$/C, which may be attributed to the weaker intensity of the TiO_2 compared to the Ru diffraction peaks.

Fig. 2 shows typical TEM images of freshly prepared $Ru_{85}Se_{15}$/C catalyst (a) and $Ru_{85}Se_{15}/TiO_2$/C catalyst (b). Nanoparticles of both the two catalysts are well dispersed on the support surfaces in a good uniformity. As shown in Fig. 3(a) and (b), the histograms denote the particle size distributions for the two catalysts. By calculating 200 randomly chosen particles in the magnified TEM images, the mean particle size for $Ru_{85}Se_{15}$/C catalyst is obtained as 1.2 nm. And particle size of $Ru_{85}Se_{15}/TiO_2$/C catalyst is almost the same as that of $Ru_{85}Se_{15}$/C catalyst.

3.2. Durability of catalysts

The polarization curves obtained from RDE test with rotation speed of 1600 rpm were used to evaluate the ORR activities of both $Ru_{85}Se_{15}$/C and $Ru_{85}Se_{15}/TiO_2$/C catalysts before and after the electrochemical durability test. The current–potential plots in Fig. 4 depict a great similarity of initial activities but a big difference between the final for the two catalysts. Little difference between the initial activities of the two catalysts may be attributed to a similar crystalline structure and catalytic site density, which is corresponding with the results from XRD and TEM analysis. Therefore, a small quantity of TiO_2 barely affects the ORR activity of the catalyst. However, the existence of TiO_2 may provide a benefit for hampering the degradation of catalytic activity. The final potential values of $Ru_{85}Se_{15}$/C and $Ru_{85}Se_{15}/TiO_2$/C are 339 mV and 476 mV vs. RHE at 2 mA cm^{-2}, respectively. It may illuminate that the inter-

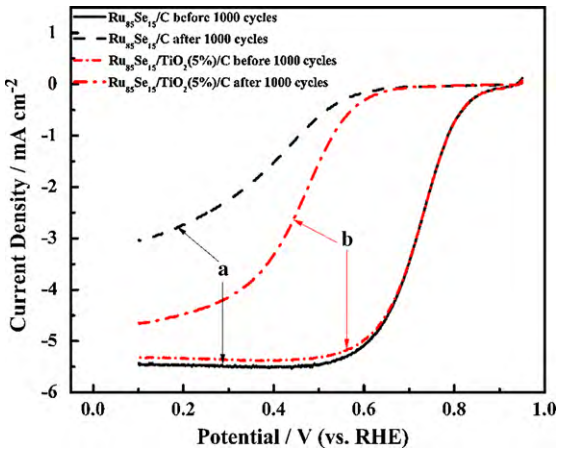

Fig. 4. ORR polarization curves before and after the electrochemical durability test (a) $Ru_{85}Se_{15}$/C catalyst and (b) $Ru_{85}Se_{15}/TiO_2$/C catalyst. Rotation speed: 1600 rpm; sweep rate: 5 mV s^{-1}.

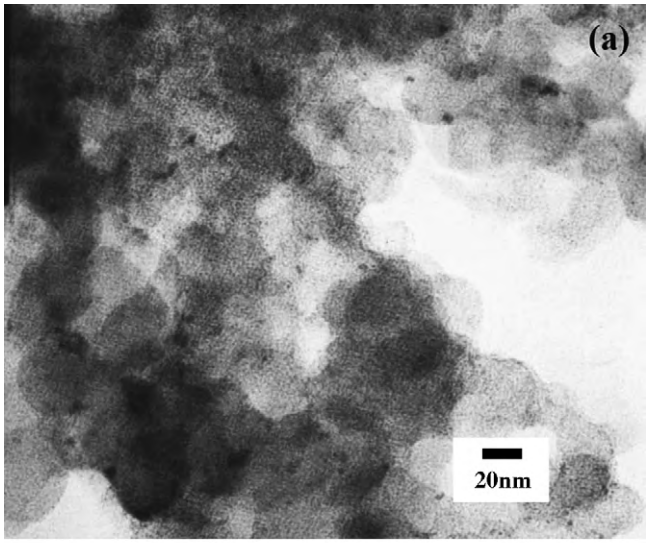

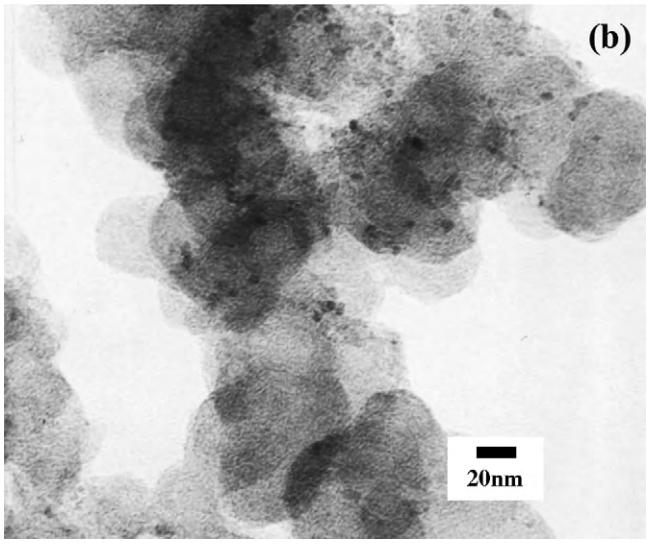

Fig. 5. TEM images of the catalysts after the electrochemical durability test (a) $Ru_{85}Se_{15}$/C catalyst and (b) $Ru_{85}Se_{15}/TiO_2$/C catalyst.

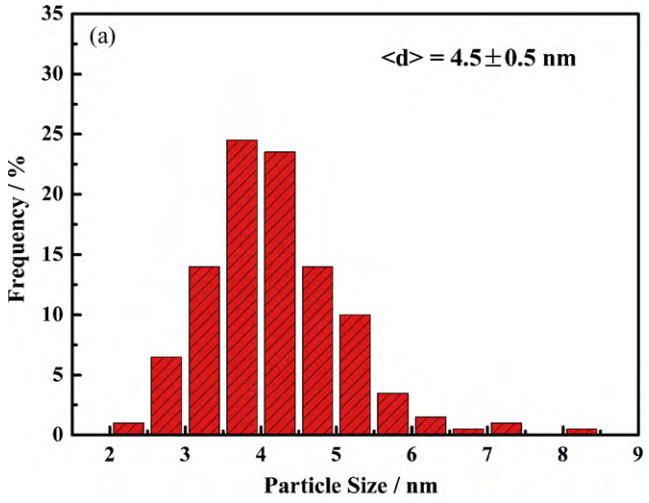

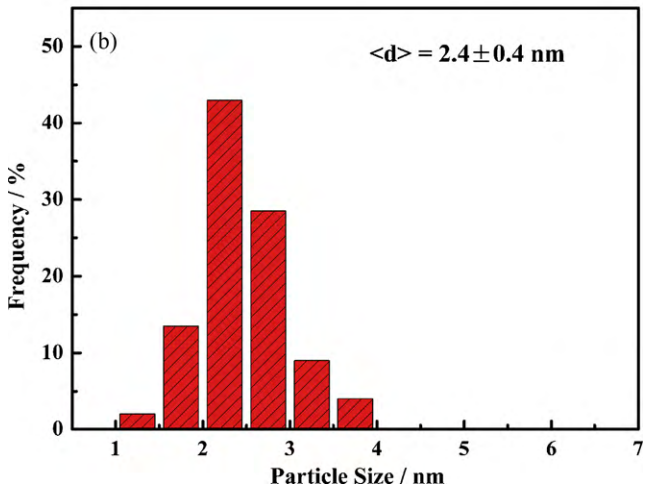

Fig. 6. Histograms of particle size distributions of the catalysts after the electrochemical durability test (a) $Ru_{85}Se_{15}$/C catalyst and (b) $Ru_{85}Se_{15}/TiO_2$/C catalyst.

action between TiO_2 and $Ru_{85}Se_{15}$ prevents catalyst particles from aggregation and oxidation.

The TEM images of the $Ru_{85}Se_{15}$/C catalyst and $Ru_{85}Se_{15}/TiO_2$/C catalyst after the electrochemical durability test are displayed in Fig. 5(a) and (b). The corresponding histograms are shown in Fig. 6(a) and (b). It is obvious that both catalysts present the agglomerations of metal nanoparticles, and the distributions of particle size are quite broader than the initial distribution. The average particle size of $Ru_{85}Se_{15}/TiO_2$/C is 2.4 nm, which is much smaller than that of $Ru_{85}Se_{15}$/C (4.5 nm). For $Ru_{85}Se_{15}$/C catalyst, the distribution of particle size is broader than that of $Ru_{85}Se_{15}/TiO_2$/C, and the agglomeration is much severer. As reported, TiO_x could avoid the agglomeration of metal particles, effectively disperse and control the nanostructure of catalysts [13]. Moreover, the catalyst crystallite can be prevented from aggregating to some extent with the existence of oxide or hydroxide, which leads to the alleviation of the catalyst aggregating [14–16]. The highly dispersed $Ru_{85}Se_{15}$ could be obstructed by the adjacent TiO_2, and the anchoring and steric hindrance effect of TiO_2 may inhibit the $Ru_{85}Se_{15}$ particles from agglomerating. The results are consistent with the results of the electrochemical durability test, which shows that $Ru_{85}Se_{15}/TiO_2$/C maintains higher final ORR activity than $Ru_{85}Se_{15}$/C.

The loss amounts of Ru and Se for the two catalysts in the electrochemical durability test were analyzed by ICP-AES. The results indicate that after the electrochemical durability

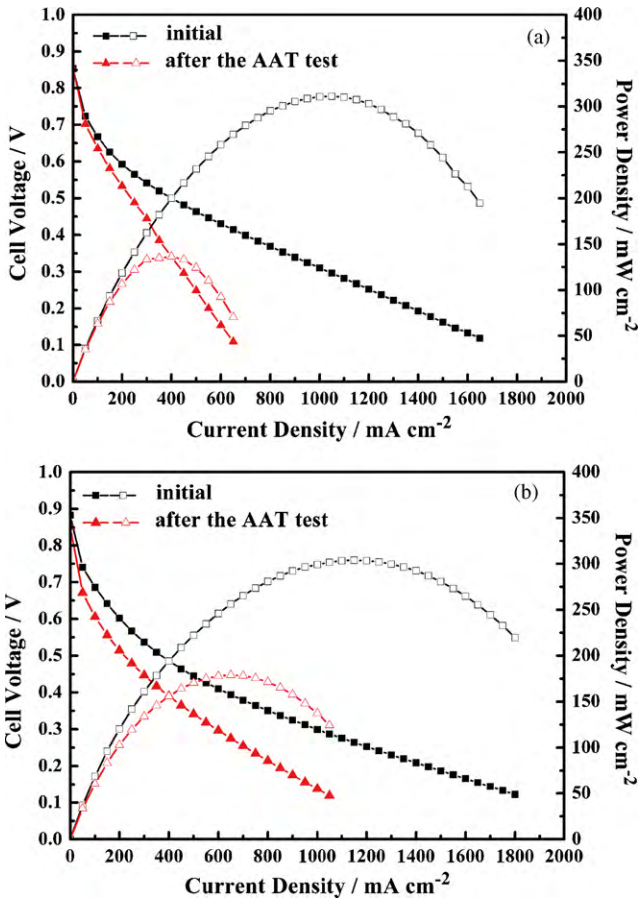

Fig. 7. Cell performances of (a) $Ru_{85}Se_{15}$/C MEA and (b) $Ru_{85}Se_{15}/TiO_2$/C MEA before and after the AAT for 1000 cycles between 0.6 and 1.0 V vs. RHE. Anode: the commercial TKK-28.4% Pt/C catalyst with Pt loading 0.4 mg cm^{-2}. Cathode: Ru loading 0.5 mg cm^{-2}. $T_{H2}/T_{cell}/T_{O2}$ = 90 °C/80 °C/85 °C, H_2/O_2 = 0.2 MPa. Membrane: Nafion 212.

test, the content of Ru element is detected as 0.0953 mg L^{-1} for the $Ru_{85}Se_{15}$/C catalyst in the 0.5 M H_2SO_4 electrolyte, and 0.0899 mg L^{-1} for the $Ru_{85}Se_{15}/TiO_2$/C catalyst. The content of Se element is 0.0274 mg L^{-1} for the $Ru_{85}Se_{15}$/C catalyst, but no Se can be detected for the $Ru_{85}Se_{15}/TiO_2$/C catalyst. The results from Zaikovskii's group [6] denote that the ORR activity of Ru_xSe_y catalyst is related to the inhibition of Ru oxidation, and Se element strongly influences their susceptibility to oxidation: the higher the amount of Se, the lower the extent of Ru oxidation. However, Se is easily lost at potential as high as 0.85 V (vs. RHE) [7]. Hence, the inhibition for the loss of Se plays a significant role in protecting Ru from oxidation. For $Ru_{85}Se_{15}/TiO_2$/C catalyst, there is no Se content loss during the electrochemical durability test, which indicates that the TiO_2 can enhance the stability of Se under high potential and consequently result in less Ru atoms oxidized than that of $Ru_{85}Se_{15}$/C catalyst. As the antioxidant of Ru, Se may be prevented from losing due to the interaction between TiO_2 and $Ru_{85}Se_{15}$. Consequently, $Ru_{85}Se_{15}/TiO_2$/C catalyst presents better stability with the addition of TiO_2.

3.3. Stability of single cell tests

Fig. 7 shows single cell performance before and after the AAT employing $Ru_{85}Se_{15}$/C and $Ru_{85}Se_{15}/TiO_2$/C as cathode electrocatalysts, respectively. It is obvious that the two single cells reveal similar initial performance. At 500 mA cm^{-2}, the power density is 231 mW cm^{-2} for $Ru_{85}Se_{15}$/C catalyst and 226 mW cm^{-2} for $Ru_{85}Se_{15}/TiO_2$/C catalyst. However, the final curves of the two single cells are evidently different. After the AAT the power densities of $Ru_{85}Se_{15}/TiO_2$/C and $Ru_{85}Se_{15}$/C MEA are 171 and 124 mW cm^{-2} at 500 mA cm^{-2}, respectively. The maximum power density of the single cell with $Ru_{85}Se_{15}/TiO_2$/C MEA is 179 mW cm^{-2}, which is also higher than that of the single cell with $Ru_{85}Se_{15}$/C MEA (136 mW cm^{-2}). It also demonstrates the effect of TiO_2 for the stability improvement of the catalyst. The TiO_2 surrounding the active metal atoms can disperse the $Ru_{85}Se_{15}$ complex nanoparticles and prevent their agglomerations. Furthermore, the existence of TiO_2 also inhibits the loss of Se, which releases catalytic devitalization of Ru by decreasing the amount of oxidation. Therefore, the single cell with $Ru_{85}Se_{15}/TiO_2$/C on the cathode presents better stability than that with $Ru_{85}Se_{15}$/C due to the addition of TiO_2. However, the detailed mechanism of the interaction between TiO_2 and $Ru_{85}Se_{15}$ is still not quite clear. Therefore, the further investigation is needed urgently.

4. Conclusions

The introduction of TiO_2 to carbon supported $Ru_{85}Se_{15}$ nanoparticles provides a favorable influence on the electrochemical stability to a certain extent, but with little impact upon crystalline structure and initial ORR activity. The existence of TiO_2 may inhibit $Ru_{85}Se_{15}$ nanoparticles from aggregation due to its anchoring and steric hindrance effect. The interaction between TiO_2 and $Ru_{85}Se_{15}$ is beneficial to stabilize Se which is regarded as the excellent antioxidant for Ru. Further research will be conducted on the detailed mechanism of the interaction between TiO_2 and $Ru_{85}Se_{15}$.

Acknowledgements

The authors gratefully appreciate the financial support by the National High Technology Research and Development Program of China (863 Program, No. 2007AA05Z129).

References

[1] N. Vante, H. Tributsch, Nature 323 (1986) 431.
[2] W. Vogel, P. Kaghazchi, T. Jacob, N. Vante, J. Phys. Chem. C 111 (2007) 3908.
[3] C. Delacôte, A. Bonakdarpour, C. Johnston, P. Zelenay, A. Wieckowski, Faraday Discuss. 140 (2009) 1.
[4] G. Liu, H. Zhang, J. Hu, Electrochem. Commun. 9 (2007) 2643.
[5] M. Shen, S. Chiao, D. Tsai, D. Wilkinson, J. Jiang, Electrochim. Acta 54 (2009) 4297.
[6] V. Zaikovskii, K. Nagabhushana, V. Kriventsov, K. Loponov, S. Cherepanova, R. Kvon, H. Bö1nnemann, D. Kochubey, E. Savinova, J. Phys. Chem. B 110 (2006) 6881.
[7] M. Solaliendres, A. Manzoli, G. Salazar-Banda, K. Eguiluz, S. Tanimoto, S. Machado, J. Solid State Electrochem. 12 (2008) 679.
[8] X. Li, C. Liu, W. Xing, T. Lu, J. Power Sources 193 (2009) 470.
[9] N. Rajalakshmi, N. Lakshmi, K. Dhathathreyan, Int. J. Hydrogen Energy 33 (2008) 7521.
[10] A. Bauer, K. Lee, C. Song, Y. Xie, J. Zhang, R. Hui, J. Power Sources 195 (2010) 3105.
[11] L. Yu, X. Qiu, J. Xi, W. Zhu, L. Chen, Electrochim. Acta 51 (2006) 6406.
[12] L. Kao, T. Hsu, K. Cheng, J. Colloid Interface Sci. 341 (2010) 359.
[13] J. Chen, S. Sarma, C. Chen, M. Cheng, S. Shih, G. Wang, J. Power Sources 159 (2006) 29.
[14] L. Feins, J. Denling, C. Wan, R. Farrauto, Eur. Patent No. 097,508 (1984).
[15] G. Liu, H. Zhang, H. Zhong, J. Hu, D. Xu, Z. Shao, Electrochim. Acta 51 (2006) 5710.
[16] W. Chen, G. Sun, J. Guo, X. Zhao, S. Yan, J. Tian, S. Tang, Z. Zhou, Q. Xin, Electrochim. Acta 51 (2006) 2391.